Frontiers of Information Technology & Electronic Engineering
www.jzus.zju.edu.cn; engineering.cae.cn; www.springerlink.com
ISSN 2095-9184 (print); ISSN 2095-9230 (online)
E-mail: jzus@zju.edu.cn

Polynomial robust observer implementation based passive synchronization of nonlinear fractional-order systems with structural disturbances

Alain Soup Tewa KAMMOGNE[†‡1], Michaux Noubé KOUNTCHOU[2], Romanic KENGNE[1], Ahmad Taher AZAR[†3,4], Hilaire Bertrand FOTSIN[1], Soup Teoua Michael OUAGNI[5]

[1]*LAMACETS, Faculty of Sciences, University of Dschang, P.O. Box 96, Cameroon*

[2]*Nuclear Technology Section, Institute of Geological and Mining Research, P.O. Box 4110, Yaoundé, Cameroon*

[3]*Robotics and Internet-of-Things Lab (RIOTU), Prince Sultan University, Riyadh 11586, Saudi Arabia*

[4]*Faculty of Computers and Artificial Intelligence, Benha University, Benha 13511, Egypt*

[5]*Laboratoire de Mécanique et de Modélisation des Systèmes Physique, Faculty of Sciences, University of Dschang, P.O. Box 96, Cameroon*

[†]E-mail: kouaneteoua@yahoo.fr; aazar@psu.edu.sa; ahmad.azar@fci.bu.edu.eg

Received Aug. 24, 2019; Revision accepted May 17, 2020; Crosschecked Aug. 5, 2020

Abstract: A robust polynomial observer is designed based on passive synchronization of a given class of fractional-order Colpitts (FOC) systems with mismatched uncertainties and disturbances. The primary objective of the proposed observer is to minimize the effects of unknown bounded disturbances on the estimation of errors. A more practicable output-feedback passive controller is proposed using an adaptive polynomial state observer. The distributed approach of a continuous frequency of the FOC is considered to analyze the stability of the observer. Then we derive some stringent conditions for the robust passive synchronization using Finsler's lemma based on the fractional Lyapunov stability theory. It is shown that the proposed method not only guarantees the asymptotic stability of the controller but also allows the derived adaptation law to remove the uncertainties within the nonlinear plant's dynamics. The entire system using passivity is implemented with details in PSpice to demonstrate the feasibility of the proposed control scheme. The results of this research are illustrated using computer simulations for the control problem of the fractional-order chaotic Colpitts system. The proposed approach depicts an efficient and systematic control procedure for a large class of nonlinear systems with the fractional derivative.

Key words: Robust passive observer; Adaptive synchronization; Lyapunov theory; Fractional-order; Polynomial observer; Uncertain parameters; H_∞-performance
https://doi.org/10.1631/FITEE.1900430 **CLC number:** TP273; O415

1 Introduction

In many engineering problems, different approaches used in controlling nonlinear systems can be more easily understood using fractional-order derivatives (Podlubny, 1999; Dasgupta et al., 2015). Since the discovery of fractional derivatives in the 16th century, the theory of equations with non-integer-order derivatives has remained a broad field of applied science that has been widely explored (Li CP and Deng, 2007; Aghababa, 2012b). Fractional-order systems have been applied in many related areas such as economics, engineering, physics, electrical engineering, robotics, control systems, chemistry, and bioengineering, and there is still no doubt about other

‡ Corresponding author
ORCID: Alain Soup Tewa KAMMOGNE, https://orcid.org/0000-0003-0234-8652; Ahmad Taher AZAR, https://orcid.org/0000-0002-7869-6373

pure science areas (Ghoudelbourk et al., 2016; Azar et al., 2018a, 2018b; Ammar et al., 2019; Djeddi et al., 2019). This is because many real systems can be more clearly described and easily modeled using a fractional-order derivative compared to integer derivatives. One of the important areas of application for our case study is in chaos theory and its control (Tavazoei and Haeri, 2007, 2008; Azar et al., 2017a, 2017b). Since Carroll and Pecora introduced synchronization of two chaotic systems with integer order, fractional-order systems have received special interest among scientists and wide interest in information security, process control, and system modeling among others (Pecora and Carroll, 1990; Aghababa, 2012a; Chen et al., 2012; Rabah et al., 2018). The analysis of nonlinear coupled systems with fractional-order derivatives is an important area of research for detailed understanding of the various complexities of emerging dynamics in real systems. Most research today is predominantly linked to neural networks, but it is worthwhile to mention that the synchronization of coupled systems remains a benchmark of all topologies encountered in the literature survey (Kammogne et al., 2019). Several synchronization techniques have been proposed in the literature, such as sliding mode control (Zhang and Yang, 2013; Aghababa, 2014, 2015a; Vaidyanathan and Azar, 2015a, 2015b; Vaidyanathan et al., 2015, 2019), the state observer (Kammogne et al., 2013; Wang et al., 2013), linear and nonlinear methods (Li C et al., 2013), passive methods (Song QK and Wang, 2010; Song J and He, 2015; Issakhov and Baitureyeva, 2018), adaptive control (Vaidyanathan and Azar, 2016a, 2016b), and the Lyapunov method (Li TZ et al., 2017), which have been applied with success to the synchronization of chaos.

In addition, the idea of passivity provides an effective method for the study of nonlinear processes, and has drawn research interest in recent years. The concept of passivity allows the stability of the system to be maintained, which is the main property of this theory. The Lyapunov-Krasovskii functional method has been used in several studies analyzing the robust synchronization of nonlinear fractional-order systems (Shen and Lam, 2014; Song S et al., 2017; Khan et al., 2020a, 2020b). Recently, finite-time passivity and passification for stochastic time-delayed Markovian switching systems with partly known transition rates were proposed by Qi et al. (2016), while Song J and He (2015) proposed a finite-time robust passive controller for a class of uncertain Lipschitz nonlinear systems with time delays. Finite-time non-fragile passivity control for neural networks was developed by Rajavel et al. (2017). Kuntanapreeda (2016) proposed adaptive control of fractional-order unified chaotic systems using a passivity-based control approach. Recently, Thuan et al. (2019) studied the robust finite-time passivity for fractional-order neural networks with uncertainties. Song QK and Wang (2010) proposed a mixed H_∞/passive projective synchronization method for fractional-order neural networks with uncertain parameters and delays.

From the above literature survey, it is noted that the robustness of the control scheme is basically linked to many constraints required by the strategy. On the other hand, many control schemes depict poorer performance and less efficiency when a complex noisy environment is considered in the calculation. It is also remarked that most of the results mentioned above and others encountered in the literature (Li LL and Yao, 2014; Sun et al., 2017; Noun and Botmart, 2018) deal more with both passive stability of neural networks and a standard class of dynamical systems (unified chaotic, Lorenz system, power chaotic systems) with fractional derivative order. However, some nonlinear system topologies, such as the Colpitts oscillator, present many important features (fractals, bifurcations, coexistence, and so on) that provide an additional specification on the control scheme. Strictly speaking, the Colpitts oscillator family presents better spectral properties that are suitable for communication application.

It is worth remembering that describing a chaotic system in observation design provides added freedom that allows the efficiency of synchronization of steady-state errors to be controlled. Note that a derivative-order system can be realized to change the synchronization effect to the extent that the polynomial viewer benefits. Also, note that the system's derivative order and polynomial observer gains can automatically be configured to resolve the synchronization effect.

In the modeling process, the modeling error creates a large number of uncertainties that can not only degrade the efficiency of the control system but also lead to dynamic system instability. Thus, the

dynamic environment is taken into account in the control design to improve the closed-loop system performance of the fractional-order system.

Furthermore, the consideration of these factors in the controller's algorithm development provides fundamental concepts for designing robust controllers. As mentioned earlier, the passivity control method has been reported for uncertain integer-order linear and nonlinear systems. The techniques developed are based on the linear matrix inequality (LMI) to the best of our knowledge. It is very difficult and unpredictable to control the LMI with unknown parameters (for example, the loop gain or the Lipschitz constant cannot be infinite in spite of the perturbations or the uncertainties in the system). In fact, controlling the nonlinear effect in the control scheme will make the observer structure considerably more complicated, and requires extra control effort. Therefore, the main contributions of this paper are based on the modern robust control technique and significant results regarding recent developments. Our contributions can be listed as follows:

1. A polynomial robust observer is designed by means of algebraic manipulation, adaptation laws, and passivity theory for synchronization of a general class of uncertain fractional nonlinear systems.

2. Synchronization robustness is evaluated in terms of the control effort, which enables the drive-response system to have a coupling speed cost.

3. A method is proposed to attenuate unmatched disturbances in fractional systems.

4. The control scheme is implemented in PSpice.

To the best of our knowledge, this is the first time that a method has been proposed to attenuate unmatched disturbances in fractional systems. A robust polynomial observer is used in this study to evaluate the observability condition based on differential algebraic parameters. Considering the complex environment, our proposed synchronization approach is best suited to actual applications.

2 Some fundamental properties of fractional derivatives

Some fundamental lemmas and definitions of fractional-order derivatives are discussed.

Definition 1 (Podlubny, 1999) For any real number n denoting the n^{th} derivative of $\varphi(t)$, D_t^q is used as a Caputo fractional differential operator. The differentiation of $\varphi(t)$ with fractional order q is established as follows:

$$D_t^{\alpha}\varphi(t)=\frac{1}{\Gamma(n-\alpha)}\int_{t_0}^{t}\varphi^{(n)}(\tau)(t-\tau)^{n-\alpha-1}\mathrm{d}\tau. \quad (1)$$

Lemma 1 (Skelton et al., 1998; de Oliveira and Skelton, 2000) Let $\boldsymbol{\eta}(t)\in\mathbb{R}^n$, $\boldsymbol{Q}\in\mathbb{R}^{n\times n}$, $\boldsymbol{G}\in\mathbb{R}^{s\times n}$, and rank($\boldsymbol{G}$)<$n$. Then,

$$\boldsymbol{\eta}^{\mathrm{T}}\boldsymbol{Q}\boldsymbol{\eta}<0,\ \forall\boldsymbol{\eta}\neq\boldsymbol{0}\ \text{such that}\ \boldsymbol{G}\boldsymbol{\eta}=\boldsymbol{0} \quad (2)$$

is satisfied if and only if under the following conditions:

1. $\boldsymbol{G}_{\pi}^{\mathrm{T}}\boldsymbol{Q}\boldsymbol{G}_{\pi}<0$, where $\boldsymbol{G}_{\pi}$ is such that $\boldsymbol{G}\boldsymbol{G}_{\pi}=\boldsymbol{0}$, and $\boldsymbol{G}\boldsymbol{G}^{\mathrm{T}}+\boldsymbol{G}_{\pi}^{\mathrm{T}}\boldsymbol{G}_{\pi}>0$, where $\boldsymbol{G}_{\pi}$ is any basis of the right null space of $\boldsymbol{G}$.

2. $\exists\rho\in\mathbb{R}$: $\boldsymbol{Q}-\rho\boldsymbol{G}^{\mathrm{T}}\boldsymbol{G}<0$.

3. $\exists\boldsymbol{V}\in\mathbb{R}^{n\times s}$: $\boldsymbol{Q}+\boldsymbol{V}\boldsymbol{G}+\boldsymbol{G}^{\mathrm{T}}\boldsymbol{V}^{\mathrm{T}}<0$.

Lemma 2 (Gai et al., 2016) Consider a fractional-order system as follows:

$$\begin{cases}D_t^q\bar{x}(t)=\varphi(t,\bar{y}(t)),\ 0\le t\le\beta,\\ \bar{x}^{(r)}(0)=\bar{x}_0^{(r)},\ r=0,1,...,m-1,\end{cases} \quad (3)$$

where $\varphi(t,\bar{y}(t))\in\mathbb{R}$ is a continuous linear frequency-distributed system. The frequency-distributed state $f(\omega, t)\in\mathbb{R}$ satisfies

$$\frac{\partial f(\omega,t)}{\partial t}=-\omega f(\omega,t)+\varphi(t,\bar{y}(t)), \quad (4)$$

where $\varphi(t,\bar{y}(t))$ is the weighted integral defined as follows:

$$\varphi(t,\bar{y}(t))=\int_0^{\infty}\mu_q(\omega)f(\omega,t)\mathrm{d}\omega, \quad (5)$$

and the frequency weighting function is given by

$$\mu_q(\omega')=\frac{q}{\omega'^{q}}\sinh(q\pi). \quad (6)$$

3 Problem formulation

3.1 Preliminaries

The state formulation of the fractional-order system is defined as follows:

$$\begin{cases} D^q \boldsymbol{x}(t) = (\boldsymbol{A} + \Delta\boldsymbol{A})\boldsymbol{x}(t) + f(\boldsymbol{x}(t)) + \bar{\boldsymbol{G}}\varsigma(t), \\ \tilde{\boldsymbol{y}}(t) = \boldsymbol{C}\boldsymbol{x}(t), \end{cases} \tag{7}$$

where $\boldsymbol{x}\in\mathbb{R}^n$ are the state variables and $\tilde{\boldsymbol{y}}\in\mathbb{R}^m$ are the measurable output vectors of system (7). $\boldsymbol{A}\in\mathbb{R}^{n\times n}$ and $\boldsymbol{C}\in\mathbb{R}^{m\times n}$ are known matrices such that ($\boldsymbol{A}$, $\boldsymbol{C}$) is observable. $\bar{\boldsymbol{G}}\in\mathbb{R}^n$. $f:\mathbb{R}^n\to\mathbb{R}^n$ is a smooth vector mapping. $\varsigma(t)\in\Im_\infty[0,\infty)$ refers to unknown external disturbances and $\Delta\boldsymbol{A}(t)$ are uncertain terms constituting the unmodeled dynamics. $\boldsymbol{q}=(q_1, q_2, \ldots, q_n)$ are the fractional orders for $0<q_i<1$ ($i=1, 2, \ldots, n$).

Assumption 1 The triplet $(\boldsymbol{A},\bar{\boldsymbol{G}},\boldsymbol{C})$ satisfies the minimum-phase assumption, i.e., $\forall\sigma\in\mathbb{C}$, $i=1, 2, \ldots, n$, $\operatorname{rank}\begin{bmatrix}\sigma\boldsymbol{I}_n-\boldsymbol{A} & \bar{\boldsymbol{G}}\\ \boldsymbol{C} & \boldsymbol{0}\end{bmatrix}=n+\operatorname{rank}(\bar{\boldsymbol{G}})$, $|\arg(\sigma)|\le\alpha_i\pi/2$, with α_i being a positive integer.

Assumption 2 $\Delta\boldsymbol{A}$ represents the time-varying system uncertainty matrix with a suitable dimension defined as follows:

$$\Delta\boldsymbol{A}=\boldsymbol{D}\boldsymbol{T}(\boldsymbol{x},t)\bar{\boldsymbol{D}}, \tag{8}$$

where $\boldsymbol{D}$ and $\bar{\boldsymbol{D}}$ are constant matrices to be adopted by the designer and $\boldsymbol{T}(\boldsymbol{x}, t)$ is a known time-varying matrix which is Lebesque measurable in t and satisfies

$$\boldsymbol{T}^{\mathrm{T}}(\boldsymbol{x},t)\boldsymbol{T}(\boldsymbol{x},t)\le\boldsymbol{I},\ \ \forall t\in[0,\infty), \tag{9}$$

where $\boldsymbol{I}$ is the identity matrix.

Assumption 3 The nonlinear vector function $\varphi(\boldsymbol{x}(t))$ is λ-Lipschitz if for an arbitrary constant $\lambda_i>0$, the following condition is satisfied:

$$\left|\varphi(\boldsymbol{x})-\varphi(\hat{\boldsymbol{x}})\right|\le\sum_{i=1}^{n}\lambda_i\left\|x_i-\hat{x}_i\right\| \tag{10}$$

Lemma 3 Consider matrices $\boldsymbol{\Lambda}$ and $\bar{\boldsymbol{\Lambda}}$ with compatible dimensions. The following inequality is satisfied for any positive constant ε_1:

$$\boldsymbol{\Lambda}^{\mathrm{T}}\bar{\boldsymbol{\Lambda}}+\bar{\boldsymbol{\Lambda}}^{\mathrm{T}}\boldsymbol{\Lambda}\le\varepsilon_1\boldsymbol{\Lambda}^{\mathrm{T}}\boldsymbol{\Lambda}+\varepsilon_1^{-1}\bar{\boldsymbol{\Lambda}}^{\mathrm{T}}\bar{\boldsymbol{\Lambda}}. \tag{11}$$

3.2 Robust passivity-observer design

This subsection presents some conditions for the robustness of an adaptive robust observer. Consider the observer of the following form:

$$\begin{cases} D^q\hat{\boldsymbol{x}}(t)=(\boldsymbol{A}+\Delta\boldsymbol{A})\hat{\boldsymbol{x}}(t)+\varphi(\hat{\boldsymbol{x}}(t))\\ \quad\quad +\boldsymbol{L}\big(\boldsymbol{y}(t)-\boldsymbol{C}\hat{\boldsymbol{x}}(t)\big)+\bar{\boldsymbol{G}}\boldsymbol{d}(t)+\boldsymbol{u}_{\mathrm{f}}(t),\\ \hat{\boldsymbol{y}}(t)=\boldsymbol{C}\hat{\boldsymbol{x}}(t), \end{cases} \tag{12}$$

where $\hat{\boldsymbol{x}}\in\mathbb{R}^n$ are the system states and $\hat{\boldsymbol{y}}\in\mathbb{R}^m$ are the estimation measurement output vectors of system (12). The switching function $\boldsymbol{d}(t)$ is the disturbance input and $\boldsymbol{L}$ is the designed matrix. $\boldsymbol{u}_{\mathrm{f}}(t)$ is a nonlinear input vector for the observer system.

Our objective is to construct a suitable controller $\boldsymbol{u}_{\mathrm{f}}(t)$ that allows the trajectory of observer system (12) to asymptotically approach the trajectory of system (7) and eventually perform the synchronization.

Definition 2 For the external nonlinear input $\boldsymbol{u}_{\mathrm{f}}(t)$ and output $\boldsymbol{y}_{\mathrm{e}}(t)$, system (7) subjected to disturbances and uncertainties is said to be passive if for any two nonnegative constants $\hbar$ and $\hat{\lambda}$ the following relationship holds:

$$\int_0^t\boldsymbol{u}_{\mathrm{f}}^{\mathrm{T}}(t)\boldsymbol{y}_{\mathrm{e}}(t)\mathrm{d}t+\hbar\ge\int_0^t s(\boldsymbol{x}(t))\mathrm{d}t-\hat{\lambda}^2\int_0^t r(t)\mathrm{d}t,\ \ \forall t\ge0, \tag{13}$$

where $s(\boldsymbol{x}(t))$ is a semi-definite function, $r(t)$ is a nonnegative function, and $\boldsymbol{y}_{\mathrm{e}}(t)=\boldsymbol{y}(t)-\hat{\boldsymbol{y}}(t)$. The energy of system (12) is closely related to the power supply from the external source. Indeed, the amount of supplied energy cannot be greater than that of the stored energy. This is the meaning of a physical system. Any system that maintains this property is objectively stable.

Corollary 1 (Byrnes et al., 1991) In the case where the disturbances and unmodeled dynamics are not considered ($\Delta\boldsymbol{A}\approx\boldsymbol{0}$ and $\varsigma(t)=\boldsymbol{d}(t)\approx\boldsymbol{0}$), inequality (13) becomes

$$\int_0^t\boldsymbol{u}_{\mathrm{f}}^{\mathrm{T}}(t)\boldsymbol{y}_{\mathrm{e}}(t)\mathrm{d}t+\hbar\ge\int_0^t s(\boldsymbol{x}(t))\mathrm{d}t,\ \ \forall t\ge0. \tag{14}$$

This is a well-known mathematical definition of the passivity for an ideal system. It is straightforward to

see that system (7) is strictly passive and lossless for the conditions $s(\boldsymbol{x}(t))>0$ and $s(\boldsymbol{x}(t))=0$, respectively.

Definition 3 Consider that systems (7)–(12), when submitted to a complex noisy environment, are passive, and suppose that any infinitely differentiable function $f(\cdot)$ such that $f(0)=0$ satisfies

$$\boldsymbol{y}_{\mathrm{e}}^{\mathrm{T}}(t)f(\boldsymbol{y}_{\mathrm{e}}(t))-r(t)>0. \tag{15}$$

Hence, the nonlinear control law $\boldsymbol{u}_{\mathrm{f}}(t)=-f(\boldsymbol{y}_{\mathrm{e}}(t))$ makes system (12) asymptotically stabilize to a fixed point.

3.3 Synchronization results

The synchronization error vector is expressed as follows:

$$D^{q}\boldsymbol{e}(t)=\boldsymbol{x}(t)-\hat{\boldsymbol{x}}(t). \tag{16}$$

Based on Eq. (16), the error system can be expressed as

$$\begin{aligned}D^{q}\boldsymbol{e}(t)=&(\boldsymbol{A}-\boldsymbol{LC})\boldsymbol{e}(t)+\big(\varphi(\boldsymbol{x}(t))-\varphi(\hat{\boldsymbol{x}}(t))\big)\\&+\bar{\boldsymbol{G}}\boldsymbol{\varsigma}(t)-\bar{\boldsymbol{G}}\boldsymbol{d}(t)+\Delta\boldsymbol{A}\boldsymbol{e}(t)-\boldsymbol{u}_{\mathrm{f}}(t),\end{aligned} \tag{17}$$

where $\boldsymbol{e}(t)=[e_1(t),\ e_2(t),\ \ldots,\ e_n(t)]^{\mathrm{T}}\in\mathbb{R}^n$ are the state vectors of error system (17).

First, controller $\boldsymbol{u}_{\mathrm{f}}(t)$ is stated as follows:

$$\boldsymbol{u}_{\mathrm{f}}(t)=-\sum_{j=1}^{p}\boldsymbol{H}\big(\boldsymbol{y}-\boldsymbol{C}\hat{\boldsymbol{x}}(t)\big)^{2j-1}+\boldsymbol{\xi}(t), \tag{18}$$

where $p\in\mathbb{Z}_{+}$ is considered as an odd number and $j>1$. $\boldsymbol{\xi}(t)$ denotes the external input signal to be determined later. $\boldsymbol{H}$ represents the adaptive control strength gain matrix with elements chosen according to the rules:

$$\dot{k}_{1i}(t)=k_i(0)\sum_{j=1}^{n}e_j(t)P_{ij}e_i(t), \tag{19}$$

where $k_i(0)$ are positive constants.

Remark 1 The nonlinear input signal $\boldsymbol{u}_{\mathrm{f}}(t)$ achieves passivity with respect to signal $\boldsymbol{y}(t)$. We define

$$\boldsymbol{y}(t)=2\boldsymbol{P}\boldsymbol{e}(t). \tag{20}$$

Finally, we derive the dynamic overall observer error equation:

$$\begin{aligned}D^{q}\boldsymbol{e}(t)=&(\boldsymbol{A}-\boldsymbol{LC})\boldsymbol{e}(t)+\big(\varphi(\boldsymbol{x}(t))-\varphi(\hat{\boldsymbol{x}}(t))\big)\\&+\bar{\boldsymbol{G}}\boldsymbol{\varpi}(t)+\Delta\boldsymbol{A}\boldsymbol{e}(t)-\sum_{j=1}^{p}\boldsymbol{K}\big(\boldsymbol{y}-\boldsymbol{C}\hat{\boldsymbol{x}}(t)\big)^{2j-1}-\boldsymbol{\xi}(t),\end{aligned} \tag{21}$$

where $\boldsymbol{\varpi}(t)=\boldsymbol{\varsigma}(t)-\boldsymbol{d}(t)$.

Proposition 1 (Cho and Rajamani, 1997; Khalil, 2007; Ngouonkadi et al., 2014) Let us restrict each $\varphi(x_i(t))$ to a non-increasing and bounded function in the closed ball B_θ ($\theta>1$). It follows that

$$\frac{\sum_{i=1}^{n}\big(\varphi(x_i(t))-\varphi(\hat{x}_i(t))\big)}{\sum_{i=1}^{n}\big(x_i(t)-\hat{x}_i(t)\big)}=\delta\ll 1. \tag{22}$$

This condition also refers to Sabatier and Farges (2017), showing that the fractional models are physically inconsistent and can be viewed as differential equations describing the collective behavior of the particle's displacement on an infinite-dimensional space. It is obvious that some properties, such as the Lipschitz condition, and their direct consequences on observability and controllability, can be questionable and do not necessarily reveal the characteristics of the physical system. To consider this aspect, in this work we choose the Lipschitz constant to be small compared to 1 ($\lambda_i\ll 1$).

We derive error system (17) based on Gai et al. (2016) as

$$\begin{cases}\dfrac{\partial\boldsymbol{Z}(\omega,t)}{\partial t}=-\omega\boldsymbol{Z}(\omega,t)+\big(\boldsymbol{A}-\boldsymbol{LC}\big)\boldsymbol{e}(t)\\\qquad\qquad+\big(\varphi(\boldsymbol{x}(t))-\varphi(\hat{\boldsymbol{x}}(t))\big)+\boldsymbol{G}\boldsymbol{\varpi}(t)\\\qquad\qquad-\sum_{j=1}^{p}\boldsymbol{H}\big(\boldsymbol{y}-\boldsymbol{C}\hat{\boldsymbol{x}}(t)\big)^{2j-1}+\Delta\boldsymbol{A}\boldsymbol{e}(t)-\boldsymbol{\xi}(t),\\\boldsymbol{e}(t)=\int_0^{\infty}\boldsymbol{\mu}(t)\boldsymbol{Z}(\omega,t)\mathrm{d}\omega.\end{cases} \tag{23}$$

3.4 Observation error stability

Assumption 4 Select an appropriate matrix $\boldsymbol{L}\in\mathbb{R}^{3\times 3}$ and two matrices $\boldsymbol{P}$ and $\boldsymbol{Q}$ such that $\boldsymbol{P}=\boldsymbol{P}^{\mathrm{T}}>0$ and $\boldsymbol{Q}=\boldsymbol{Q}^{\mathrm{T}}$, which satisfy the following conditions:

$$\begin{aligned}&\boldsymbol{P}\big(\boldsymbol{A}-\boldsymbol{LC}+\boldsymbol{H}_1\boldsymbol{C}\big)+\big(\boldsymbol{A}-\boldsymbol{LC}+\boldsymbol{H}_1\boldsymbol{C}\big)^{\mathrm{T}}\boldsymbol{P}\\&-\boldsymbol{P}\boldsymbol{H}-\boldsymbol{H}^{\mathrm{T}}\boldsymbol{P}+\boldsymbol{P}\boldsymbol{D}\boldsymbol{D}^{\mathrm{T}}\boldsymbol{P}+\bar{\boldsymbol{D}}^{\mathrm{T}}\boldsymbol{D}-\gamma^{-2}\boldsymbol{I}=-\boldsymbol{Q},\end{aligned} \tag{24}$$

$$\lambda_{\min}\left(\boldsymbol{E}_i+\boldsymbol{E}_i^{\mathrm{T}}\right)\geq 0,\quad i=2,3,...,p, \tag{25}$$

with $\boldsymbol{E}_i=\boldsymbol{P}\boldsymbol{H}_i\boldsymbol{C}$.

Then, robust passivity synchronization can be obtained using controller (18) with adaptive law (19).

Theorem 1 With the aforementioned assumptions, master system (7) asymptotically synchronizes observer system (12) under conditions (18) and (19).

Proof We select the Lyapunov functional candidate for system (21) as follows:

$$V(t)=V_1(t)+V_2(t), \tag{26}$$

$$\begin{cases}V_1(t)=\int_0^{\infty}\boldsymbol{Z}^{\mathrm{T}}(\omega,t)\boldsymbol{\mu}(\omega)\boldsymbol{P}\boldsymbol{Z}(\omega,t)\mathrm{d}\omega,\\ V_2(t)=\sum_{i=1}^{n}\dfrac{1}{2k_i(0)}\left(k_i(0)-k_i\right)^2.\end{cases} \tag{27}$$

The combination of Eqs. (18), (21), and (22) gives

$$\begin{aligned}\dot{V}(t)=&\int_0^{\infty}[-\omega\boldsymbol{Z}(\omega,t)+(\boldsymbol{A}-\boldsymbol{L}\boldsymbol{C})\boldsymbol{e}(t)\\&+\left(\varphi(\boldsymbol{x}(t))-\varphi(\hat{\boldsymbol{x}}(t))\right)+\boldsymbol{G}\boldsymbol{\varpi}(t)+\Delta\boldsymbol{A}\boldsymbol{e}(t)\\&-\sum_{j=1}^{p}\boldsymbol{H}\left(\boldsymbol{y}-\boldsymbol{C}\hat{\boldsymbol{x}}(t)\right)^{2j-1}-\boldsymbol{\xi}(t)]^{\mathrm{T}}\boldsymbol{\mu}(\omega)\boldsymbol{P}\boldsymbol{Z}(\omega,t)\mathrm{d}\omega\\&+\int_0^{\infty}\boldsymbol{Z}^{\mathrm{T}}(\omega,t)\boldsymbol{\mu}(\omega)\boldsymbol{P}[\left(\boldsymbol{A}-\boldsymbol{L}\boldsymbol{C}\right)\boldsymbol{e}(t)+\left(\varphi(\boldsymbol{x}(t))-\varphi(\hat{\boldsymbol{x}}(t))\right)\\&+\boldsymbol{G}\boldsymbol{\varpi}(t)+\Delta\boldsymbol{A}\boldsymbol{e}(t)-\sum_{j=1}^{p}\boldsymbol{H}\left(\boldsymbol{y}-\boldsymbol{C}\hat{\boldsymbol{x}}(t)\right)^{2j-1}-\boldsymbol{\xi}(t)]\mathrm{d}\omega\\&+\sum_{i=1}^{n}\frac{1}{k_i(0)}\left(k_i(0)-k_i\right)^2k_i(0)\sum_{j=1}^{n}e_j(t)P_{ij}e_i(t).\end{aligned} \tag{28}$$

From Eq. (21) and inequality (25), one obtains

$$\begin{aligned}\dot{V}(t)\leq&\boldsymbol{e}^{\mathrm{T}}(t)\left[\boldsymbol{P}(\boldsymbol{A}-\boldsymbol{L}\boldsymbol{C})+(\boldsymbol{A}-\boldsymbol{L}\boldsymbol{C})^{\mathrm{T}}-\boldsymbol{P}\boldsymbol{H}-\boldsymbol{H}^{\mathrm{T}}\boldsymbol{P}\right]\boldsymbol{e}(t)\\&+2\boldsymbol{e}^{\mathrm{T}}(t)\boldsymbol{P}\varphi(\boldsymbol{e}(t))+2\boldsymbol{e}^{\mathrm{T}}(t)\boldsymbol{P}\boldsymbol{G}\boldsymbol{\varpi}(t)+2\boldsymbol{e}^{\mathrm{T}}(t)\boldsymbol{P}\Delta\boldsymbol{A}\boldsymbol{e}(t)\\&-2\sum_{j=1}^{p}\boldsymbol{H}\left(\boldsymbol{y}-\boldsymbol{C}\hat{\boldsymbol{x}}(t)\right)^{2j-1}+2\boldsymbol{e}^{\mathrm{T}}(t)\boldsymbol{P}\boldsymbol{\xi}(t).\end{aligned} \tag{29}$$

By Lemma 1, the following inequalities hold:

$$2\boldsymbol{e}^{\mathrm{T}}(t)\boldsymbol{P}\bar{\boldsymbol{G}}\boldsymbol{\varpi}(t)\leq\gamma^{-2}\boldsymbol{e}^{\mathrm{T}}(t)\boldsymbol{P}^2\boldsymbol{e}(t)+\gamma^2\boldsymbol{\varpi}^{\mathrm{T}}(t)\bar{\boldsymbol{G}}\boldsymbol{\varpi}(t), \tag{30}$$

$$2\boldsymbol{e}^{\mathrm{T}}(t)\boldsymbol{P}\Delta\boldsymbol{A}\boldsymbol{e}(t)\leq\boldsymbol{e}^{\mathrm{T}}(t)\left(\boldsymbol{P}\boldsymbol{D}\boldsymbol{D}^{\mathrm{T}}\boldsymbol{P}+\bar{\boldsymbol{D}}^{\mathrm{T}}\bar{\boldsymbol{D}}\right)\boldsymbol{e}(t), \tag{31}$$

where $\boldsymbol{\varpi}(t)=\boldsymbol{\varsigma}(t)-\boldsymbol{d}(t)$, $\varphi(\boldsymbol{e}(t))=\varphi(\boldsymbol{x}(t))-\varphi(\hat{\boldsymbol{x}}(t))$.

Substituting inequalities (30) and (31) into inequality (29), one obtains

$$\begin{aligned}\dot{V}(t)\leq&\boldsymbol{e}^{\mathrm{T}}(t)\left[\boldsymbol{P}(\boldsymbol{A}-\boldsymbol{L}\boldsymbol{C}+\boldsymbol{H}_1\boldsymbol{C})+(\boldsymbol{A}-\boldsymbol{L}\boldsymbol{C}+\boldsymbol{H}_1\boldsymbol{C})^{\mathrm{T}}\right.\\&\left.-\boldsymbol{P}\boldsymbol{H}-\boldsymbol{H}^{\mathrm{T}}\boldsymbol{P}+\boldsymbol{P}\boldsymbol{D}\boldsymbol{D}^{\mathrm{T}}\boldsymbol{P}+\bar{\boldsymbol{D}}^{\mathrm{T}}\bar{\boldsymbol{D}}-\gamma^{-2}\boldsymbol{I}\right]\boldsymbol{e}(t)\\&+2\boldsymbol{e}^{\mathrm{T}}(t)\boldsymbol{P}\varphi(\boldsymbol{e}(t))+2\boldsymbol{e}^{\mathrm{T}}(t)\boldsymbol{P}\Delta\boldsymbol{A}\boldsymbol{e}(t)\\&-\sum_{j=2}^{p}\boldsymbol{H}\left(\boldsymbol{C}\boldsymbol{e}(t)\right)^{2j-2}\boldsymbol{e}^{\mathrm{T}}(t)\left(\boldsymbol{E}_i+\boldsymbol{E}_i^{\mathrm{T}}\right)\boldsymbol{e}(t)\\&+2\boldsymbol{e}^{\mathrm{T}}(t)\boldsymbol{P}\boldsymbol{\xi}(t)+\gamma^2\boldsymbol{\varpi}^{\mathrm{T}}(t)\boldsymbol{\varpi}(t).\end{aligned} \tag{32}$$

From Assumption 3, we derive the following:

$$\begin{aligned}&\dot{V}(t)\leq-\boldsymbol{e}^{\mathrm{T}}(t)\boldsymbol{Q}\boldsymbol{e}(t)+2\boldsymbol{e}^{\mathrm{T}}(t)\boldsymbol{P}\varphi(\boldsymbol{e}(t))+2\boldsymbol{e}^{\mathrm{T}}(t)\boldsymbol{P}\Delta\boldsymbol{A}\boldsymbol{e}(t)\\&-\sum_{j=2}^{p}\boldsymbol{H}\left(\boldsymbol{C}\boldsymbol{e}(t)\right)^{2j-2}\boldsymbol{e}^{\mathrm{T}}(t)\left(\boldsymbol{E}_i+\boldsymbol{E}_i^{\mathrm{T}}\right)\boldsymbol{e}(t)\\&+2\boldsymbol{e}^{\mathrm{T}}(t)\boldsymbol{P}\boldsymbol{\xi}(t)+\gamma^2\boldsymbol{\varpi}^{\mathrm{T}}(t)\boldsymbol{\varpi}(t)\\&=\begin{bmatrix}\boldsymbol{e}(t)\\ \varphi(\boldsymbol{e}(t))\end{bmatrix}^{\mathrm{T}}\begin{bmatrix}-\boldsymbol{Q}&\boldsymbol{P}\\ \boldsymbol{P}&\boldsymbol{0}\end{bmatrix}\begin{bmatrix}\boldsymbol{e}(t)\\ \varphi(\boldsymbol{e}(t))\end{bmatrix}+2\boldsymbol{e}^{\mathrm{T}}(t)\boldsymbol{P}\boldsymbol{\xi}(t)\\&+\gamma^2\boldsymbol{\varpi}^{\mathrm{T}}(t)\boldsymbol{\varpi}(t)-\sum_{j=2}^{p}\boldsymbol{H}\left(\boldsymbol{C}\boldsymbol{e}(t)\right)^{2j-2}\boldsymbol{e}^{\mathrm{T}}(t)\left(\boldsymbol{E}_i+\boldsymbol{E}_i^{\mathrm{T}}\right)\boldsymbol{e}(t).\end{aligned} \tag{33}$$

Let $\boldsymbol{\eta}(t)=\begin{bmatrix}\boldsymbol{e}(t)\\ \varphi(\boldsymbol{e}(t))\end{bmatrix}$ and $\boldsymbol{\Sigma}=\begin{bmatrix}-\boldsymbol{Q}&\boldsymbol{P}\\ \boldsymbol{P}&\boldsymbol{0}\end{bmatrix}$, and inequality (33) becomes

$$\dot{V}(t)\leq-\boldsymbol{\eta}^{\mathrm{T}}(t)\boldsymbol{\Sigma}\boldsymbol{\eta}(t)+\boldsymbol{y}^{\mathrm{T}}(t)\boldsymbol{\xi}(t)+\gamma^2\boldsymbol{\varpi}^{\mathrm{T}}(t)\boldsymbol{\varpi}(t). \tag{34}$$

Integrating both sides of inequality (34) in the range $[0, t]$ gives

$$\begin{aligned}&V(\boldsymbol{e}(t))-V(\boldsymbol{e}(0))\leq\int_0^t\boldsymbol{\eta}^{\mathrm{T}}(\tau)\boldsymbol{\Sigma}\boldsymbol{\eta}(\tau)\mathrm{d}\tau\\&+\gamma^2\int_0^t\boldsymbol{\varpi}^{\mathrm{T}}(\tau)\boldsymbol{\varpi}(\tau)\mathrm{d}\tau+\int_0^t\boldsymbol{y}^{\mathrm{T}}(\tau)\boldsymbol{\xi}(\tau)\mathrm{d}\tau.\end{aligned} \tag{35}$$

Then, we have

$$\begin{aligned}&\int_0^t\boldsymbol{y}^{\mathrm{T}}(\tau)\boldsymbol{\xi}(\tau)\mathrm{d}\tau+V(\boldsymbol{e}(0))\geq-\int_0^t\boldsymbol{\eta}^{\mathrm{T}}(\tau)\boldsymbol{\Sigma}\boldsymbol{\eta}(\tau)\mathrm{d}\tau\\&-\gamma^2\int_0^t\boldsymbol{\varpi}^{\mathrm{T}}(\tau)\boldsymbol{\varpi}(\tau)\mathrm{d}\tau+V(\boldsymbol{e}(t)).\end{aligned} \tag{36}$$

Let $R(t)=\boldsymbol{\varpi}^{\mathrm{T}}(t)\boldsymbol{\varpi}(t)$ and consider that $V(\boldsymbol{e}(t))\geq 0$. One obtains

$$\begin{aligned}&\int_0^t \boldsymbol{y}^{\mathrm{T}}(\tau)\boldsymbol{\xi}(\tau)\mathrm{d}\tau + V(\boldsymbol{e}(0))\\ &\geq \int_0^t \boldsymbol{\eta}^{\mathrm{T}}(\tau)\boldsymbol{\Sigma}\boldsymbol{\eta}(\tau)\mathrm{d}\tau - \gamma^2\int_0^t R(\tau)\mathrm{d}\tau.\end{aligned} \tag{37}$$

The external input signal $\boldsymbol{\xi}(t)$ renders error system (17) passive under $\boldsymbol{u}_{\mathrm{f}}(t)$. Relation (37) satisfies the passivity stated in Definition 2. The proof is completed.

Theorem 2 (Zero-input error response) If $\boldsymbol{\xi}(t)=\boldsymbol{0}$, then the closed-loop error system (17) is asymptotically stable.

Proof Inequality (34) takes the following form:

$$\dot{V}(t) \leq -\boldsymbol{\eta}^{\mathrm{T}}(t)\boldsymbol{\Sigma}\boldsymbol{\eta}(t) + \gamma^2\boldsymbol{\varpi}^{\mathrm{T}}(t)\boldsymbol{\varpi}(t). \tag{38}$$

It is clear that if $\boldsymbol{\omega}(t)=\boldsymbol{0}$, then

$$\dot{V}(\boldsymbol{e}(t)) < -\lambda_{\min}(\boldsymbol{Q})\left\|\boldsymbol{\eta}(t)\right\|^2 < 0. \tag{39}$$

This establishes the global and asymptotic stability of dynamic error system (21). From Eq. (22), we have

$$\boldsymbol{\eta}(t) \to \boldsymbol{0} \text{ when } t \to \infty \text{ that is } \lim_{t\to\infty}\left\|\boldsymbol{e}(t)\right\| = 0. \tag{40}$$

If $\boldsymbol{\omega}(t)\neq\boldsymbol{0}$ and rearranging inequality (38), we have

$$\dot{V}(t) + \boldsymbol{\eta}^{\mathrm{T}}(t)\boldsymbol{\Sigma}\boldsymbol{\eta}(t) - \gamma^2\boldsymbol{\varpi}^{\mathrm{T}}(t)\boldsymbol{\varpi}(t) < 0. \tag{41}$$

This leads to

$$\dot{V}(t) \leq \begin{bmatrix}\boldsymbol{\eta}(t)\\ \boldsymbol{\varpi}(t)\end{bmatrix}^{\mathrm{T}}\begin{bmatrix}-\boldsymbol{\Sigma} & \boldsymbol{0}\\ \boldsymbol{0} & -\gamma^2\boldsymbol{I}\end{bmatrix}\begin{bmatrix}\boldsymbol{\eta}(t)\\ \boldsymbol{\varpi}(t)\end{bmatrix}. \tag{42}$$

Define a cost function $J_0(\boldsymbol{e}(t),\boldsymbol{\omega}(t))$ as follows:

$$J_0(\boldsymbol{\eta}(t),\boldsymbol{\varpi}(t)) = \dot{V}(t) + \boldsymbol{y}_{\mathrm{e}}^{\mathrm{T}}(t)\boldsymbol{y}_{\mathrm{e}}(t) - \gamma^2\boldsymbol{\varpi}^{\mathrm{T}}(t)\boldsymbol{\varpi}(t). \tag{43}$$

Substituting inequality (38) into Eq. (43) yields

$$J_0(\boldsymbol{\eta}(t),\boldsymbol{\varpi}(t)) \leq \begin{bmatrix}\boldsymbol{\eta}(t)\\ \boldsymbol{\varpi}(t)\end{bmatrix}^{\mathrm{T}}\boldsymbol{\Upsilon}\begin{bmatrix}\boldsymbol{\eta}(t)\\ \boldsymbol{\varpi}(t)\end{bmatrix}, \tag{44}$$

where

$$\boldsymbol{\Upsilon} = \begin{bmatrix}-\boldsymbol{\Sigma}+\bar{\boldsymbol{C}} & \boldsymbol{0}\\ \boldsymbol{0} & -\gamma^2\boldsymbol{I}\end{bmatrix},\ \bar{\boldsymbol{C}} = \begin{bmatrix}\boldsymbol{C}^{\mathrm{T}}\boldsymbol{C} & \boldsymbol{0}\\ \boldsymbol{0} & \boldsymbol{0}\end{bmatrix}. \tag{45}$$

Consider a positive constant δ and suppose that the following is satisfied:

$$\boldsymbol{\Upsilon}' = \boldsymbol{\Upsilon} + \begin{bmatrix}\delta\boldsymbol{P} & \boldsymbol{0}\\ \boldsymbol{0} & \boldsymbol{0}\end{bmatrix} = \begin{bmatrix}-\boldsymbol{\Sigma}+\bar{\boldsymbol{C}}+\delta\boldsymbol{P} & \boldsymbol{0}\\ \boldsymbol{0} & -\gamma^2\boldsymbol{I}\end{bmatrix} < 0. \tag{46}$$

Thus, we have

$$\begin{aligned}J_0(\boldsymbol{\eta}(t),\boldsymbol{\varpi}(t)) &\leq \begin{bmatrix}\boldsymbol{\eta}(t)\\ \boldsymbol{\varpi}(t)\end{bmatrix}^{\mathrm{T}}\boldsymbol{\Upsilon}\begin{bmatrix}\boldsymbol{\eta}(t)\\ \boldsymbol{\varpi}(t)\end{bmatrix}\\ &= \begin{bmatrix}\boldsymbol{\eta}(t)\\ \boldsymbol{\varpi}(t)\end{bmatrix}^{\mathrm{T}}\left(\boldsymbol{\Upsilon}' - \begin{bmatrix}\delta\boldsymbol{P} & \boldsymbol{0}\\ \boldsymbol{0} & \boldsymbol{0}\end{bmatrix}\right)\begin{bmatrix}\boldsymbol{\eta}(t)\\ \boldsymbol{\varpi}(t)\end{bmatrix}\\ &< -\begin{bmatrix}\boldsymbol{\eta}(t)\\ \boldsymbol{\varpi}(t)\end{bmatrix}^{\mathrm{T}}\begin{bmatrix}\delta\boldsymbol{P} & \boldsymbol{0}\\ \boldsymbol{0} & \boldsymbol{0}\end{bmatrix}\begin{bmatrix}\boldsymbol{\eta}(t)\\ \boldsymbol{\varpi}(t)\end{bmatrix} < 0,\end{aligned} \tag{47}$$

which allows us to conclude that $J_0(\boldsymbol{\eta}(t),\ \boldsymbol{\varpi}(t)) <0$. Then, error system (21) through control input $\boldsymbol{u}_{\mathrm{f}}(t)$ is asymptotically stable, and the proof of Theorem 2 is completed.

From Definition 3, $\boldsymbol{\xi}(t)=-f(\boldsymbol{y}(t))$ satisfies $f(0)=0$ and $\boldsymbol{y}_{\mathrm{e}}^{\mathrm{T}}(t)f(\boldsymbol{y}_{\mathrm{e}}(t)) > 0$ enables error system (21) to asymptotically stabilize.

Theorem 3 For any selected signal $\boldsymbol{\xi}(t)$ such as

$$\boldsymbol{\xi}(t) = -\gamma^2\boldsymbol{y}(t) = -2\gamma^2\boldsymbol{P}\boldsymbol{e}(t), \tag{48}$$

error system (21) satisfies the stability criteria.

Proof Combining inequality (38) and Eq. (48), we obtain

$$\begin{aligned}\dot{V}(t) &\leq -\boldsymbol{\eta}^{\mathrm{T}}(t)\boldsymbol{\Sigma}\boldsymbol{\eta}(t) + \gamma^2\boldsymbol{\varpi}^{\mathrm{T}}(t)\boldsymbol{\varpi}(t) - \gamma^2\boldsymbol{y}^{\mathrm{T}}(t)\boldsymbol{y}(t)\\ &= (\boldsymbol{\eta}'(t))^{\mathrm{T}}\boldsymbol{\Omega}\boldsymbol{\eta}'(t),\end{aligned} \tag{49}$$

where $\boldsymbol{\eta}'(t)=[\boldsymbol{\eta}(t),\ \boldsymbol{\varpi}(t), \boldsymbol{y}(t)]^{\mathrm{T}}$ and

$$\boldsymbol{\Omega} = \begin{bmatrix}-\boldsymbol{\Sigma} & * & *\\ \boldsymbol{0} & \gamma^2\boldsymbol{I} & *\\ \boldsymbol{0} & \boldsymbol{0} & -\gamma^2\boldsymbol{I}\end{bmatrix} = \boldsymbol{\Omega}^{\mathrm{T}}.$$

From Finsler's Lemma 1, we obtain

$$(\boldsymbol{\eta}'(t))^{\mathrm{T}}\boldsymbol{\Omega}\boldsymbol{\eta}'(t) < 0. \tag{50}$$

From inequality (47), we can easily obtain the following for the bounded disturbances:

$$\dot{V}(t) \leq -\lambda_{\min}(\boldsymbol{\Omega})\left\|\boldsymbol{\eta}'(t)\right\|^2 < 0,\ \forall\boldsymbol{\eta}'(t) \neq \boldsymbol{0}. \tag{51}$$

Then, the global error system (21) is Lyapunov stable. This ends the proof.

4 Simulation results and discussion

4.1 Fractional-order modified Colpitts oscillator

We consider the Colpitts circuit for this study. The simplified diagram of the fractional-order modified Colpitts oscillator (FMCO) is sketched in Fig. 1. Compared with the common Colpitts oscillator (Fotsin and Daafouz, 2005), the modified circuit includes an extra resistance R_d, which offers the possibility of an electronic analog or digital control on the system dynamics (Kammogne and Fotsin, 2014). This circuit uses an inductor (L) with fractional order q_3 and a pair of ultracapacitors ($c_1 = C^{q_1}$ and $c_2 = C^{q_2}$) with fractional orders q_1 and q_2, respectively.

Remark 2 In electronic design, there is no fractional component that can be implemented physically. At any frequency, the behaviors of the supposed fractional capacitances and inductor are assumed to be comparable to the behaviors of those considered as integer ones. Thus, the resulting behavior of the experimental setup in Fig. 1 is questionable in practice. Note that these components must not be modified in practice, which reduces the bandwidth of the system and causes instability in the circuit, because the highest resistance value of the fracture unit is sometimes not available.

From Fig. 1, we derive the following dimensionless state equations:

$$\begin{cases} \dfrac{\mathrm{d}^{q_1}x_1}{\mathrm{d}t^{q_1}} = x_3 - \alpha\exp(-ax_3 - bx_2), \\ \dfrac{\mathrm{d}^{q_2}x_2}{\mathrm{d}t^{q_2}} = -\beta - \beta x_2 + x_3, \\ \dfrac{\mathrm{d}^{q_3}x_3}{\mathrm{d}t^{q_3}} = 1 - x_1 - x_2 - \gamma x_3, \end{cases} \tag{52}$$

where a, b, α, β, and γ are the system's parameters. For instance, system (52) has a complex phenomenon for a specific set of values:

$$a = 2.251\,362,\ b = 192.3,\ \beta = 0.106\,481\,481\,5,$$
$$\gamma = 0.934,\ \alpha = 8.518\,518\times10^{-11}.$$

For the numerical solution of all fractional-order differential equations in this study, we use the Adams–Bashforth–Moulton method proposed by Diethelm et al. (2002). This algorithm is based on the predictor-corrector method and uses the Caputo definition of the fractional-order derivative (Aghababa, 2015b; Kengne et al., 2018; Pelap et al., 2018). Typically, for q=0.95, FMCO depicts the chaotic behavior as shown in Fig. 2.

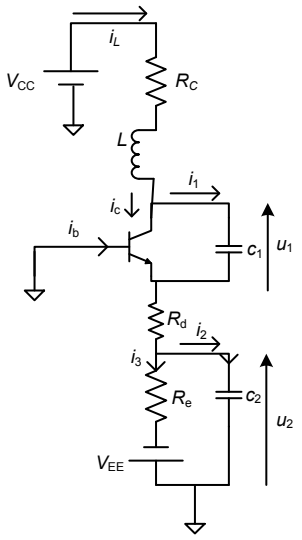

Fig. 1 Schematic circuit model of the fractional-order modified Colpitts oscillator (FMCO)

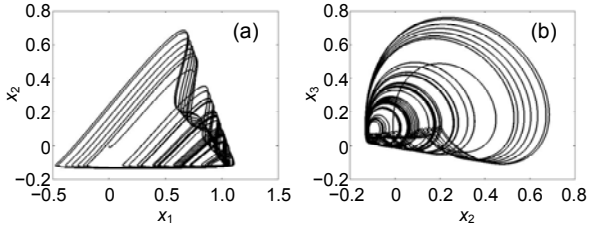

Fig. 2 Phase portraits of the fractional-order modified Colpitts oscillator (FMCO): (a) x_2 vs. x_1; (b) x_3 vs. x_2

4.2 Numerical results for robust passive synchronization

Consider Eq. (52) as follows:

$$\begin{cases} D^q\boldsymbol{x}(t) = (\boldsymbol{A} + \Delta\boldsymbol{A})\boldsymbol{x}(t) + \varphi(\boldsymbol{x}(t)) + \bar{\boldsymbol{G}}\boldsymbol{\varsigma}(t), \\ \boldsymbol{y}(t) = \boldsymbol{C}\boldsymbol{x}(t), \end{cases} \tag{53}$$

where

$$\begin{cases} \boldsymbol{A} = \begin{bmatrix} 0 & 0 & 1 \\ 0 & -\beta & 1 \\ -1 & -1 & -\gamma \end{bmatrix}, \bar{\boldsymbol{G}}\boldsymbol{\varsigma}(t) = h[d_1(t), d_2(t), d_3(t)]^{\mathrm{T}}, \\ \varphi(\boldsymbol{x}) = \begin{bmatrix} -\alpha\exp(-ax_3 - bx_2) \\ -\beta \\ 1 \end{bmatrix}, \end{cases} \tag{54}$$

and h is a positive constant. For a real-time control scheme, simply select the matrices in Eqs. (20) and (21) as

$$\boldsymbol{C}=\begin{bmatrix}1\\0\\-1\end{bmatrix},\ \boldsymbol{P}=\begin{bmatrix}1&0&0\\0&1&0\\0&0&1\end{bmatrix},\ \boldsymbol{L}=\begin{bmatrix}1&0&0\\0&1&0\\0&0&1\end{bmatrix}. \tag{55}$$

The controller takes the following form:

$$\begin{aligned}\boldsymbol{u}_{\mathrm{f}}(t)&=-\sum_{j=1}^{p}\boldsymbol{K}\left(\boldsymbol{y}-\boldsymbol{C}\hat{\boldsymbol{x}}(t)\right)^{2j-1}+\boldsymbol{\xi}(t)\\&=-\begin{bmatrix}k_{11}(e_1-e_3)+k_{21}(e_1-e_3)^3+\cdots+k_{(2p-1)1}(e_1-e_3)^{2p-1}\\k_{12}(e_1-e_3)+k_{22}(e_1-e_3)^3+\cdots+k_{(2p-1)2}(e_1-e_3)^{2p-1}\\k_{13}(e_1-e_3)+k_{23}(e_1-e_3)^3+\cdots+k_{(2p-1)3}(e_1-e_3)^{2p-1}\end{bmatrix}\\&\quad-2\gamma^2\begin{bmatrix}e_1&0&0\\0&e_2&0\\0&0&e_3\end{bmatrix}.\end{aligned} \tag{56}$$

Obviously Eq. (56) is designed to deal with unknown parameters. The appropriate control law for synchronization is given as follows:

$$\dot{k}_{1j}(t)=k_{jj}(0)\sum_{i=1}^{n}e_i(t)P_{ij}e_j(t)=\begin{bmatrix}k_{11}(0)e_1^2(t)\\k_{12}(0)e_2^2(t)\\k_{13}(0)e_3^2(t)\end{bmatrix}. \tag{57}$$

Note that this control law significantly improves the transient error response and logically improves the accuracy of steady-state tracking. The parameters of the scheme are set as follows:

$$m=2,\ h=10^{-4},\ \begin{bmatrix}k_{21}\\k_{22}\\k_{23}\end{bmatrix}=10^{-3}\begin{bmatrix}15\\6\\12\end{bmatrix}. \tag{58}$$

Parameter h represents the perturbed strength compared with the magnitude of state variables x_i (i=1, 2, 3). The time-varying parameter perturbations added to the observer system are given as follows:

$$\boldsymbol{\varsigma}(\boldsymbol{x},t)=[6\sin(5t),(7/3)\cos t,5\sin(3t)]^{\mathrm{T}}, \tag{59}$$

$$\boldsymbol{d}(\boldsymbol{x},t)=[6\cos(5t),(7/3)\sin(2t),5\cos(3t)]^{\mathrm{T}}. \tag{60}$$

The parametric uncertainties (8) can take the following form:

$$\|\boldsymbol{T}(\boldsymbol{x},t)\|\le\omega=0.085, \tag{61}$$

$$\boldsymbol{D}=\begin{bmatrix}\sin(2t)&1&0\\0&0&0\\0&-1&1\end{bmatrix},\ \bar{\boldsymbol{D}}=\begin{bmatrix}0&-1&0\\0&1&0\\0&\cos(5t)&\sin t\end{bmatrix}. \tag{62}$$

The initial conditions of the master and the slave systems are chosen as

$$(x_{10},x_{20},x_{30})=(5\times10^{-8},2\times10^{-9},7\times10^{-9}),$$
$$(\hat{x}_{10},\hat{x}_{20},\hat{x}_{30})=(5\times10^{-2},3\times10^{-3},7\times10^{-4}).$$

The derivative order considered for the simulation is q=0.95, and we notice that for this specific value, the modified Colpitts oscillator exhibits chaotic behavior (Kammogne et al., 2020). When the disturbances are not considered in the scheme, the trajectories are presented in Fig. 3. It is clear that the controller achieves complete synchronization after a short transient period. When the controller is not activated, i.e., taking $u(t)$=0, the trajectories of state variables between the master and the observer are shown in Fig. 4.

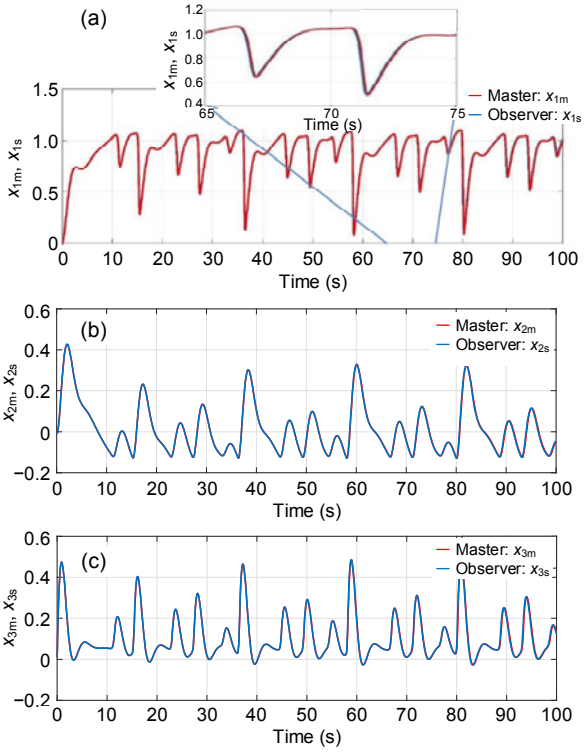

Fig. 3 Evolution of the trajectories when the disturbances are not considered: (a) $x_1(t)$, $\hat{x}_1(t)$; (b) $x_2(t)$, $\hat{x}_2(t)$; (c) $x_3(t)$, $\hat{x}_3(t)$

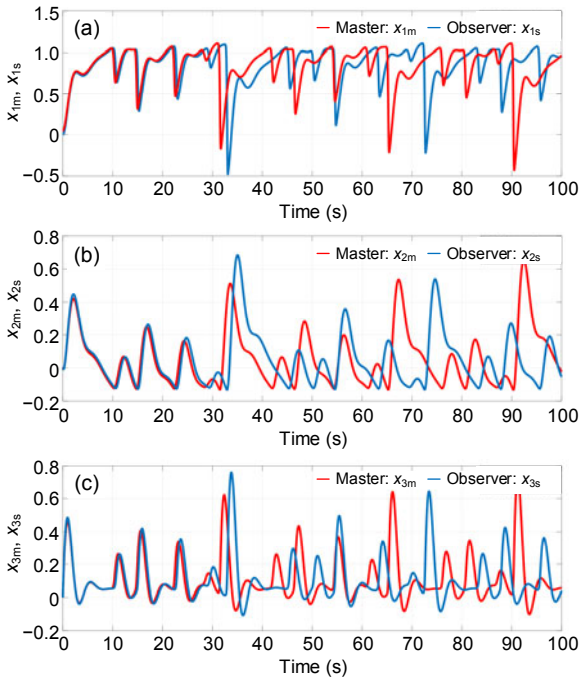

Fig. 4 Evolution of the trajectories when the controller is deactivated: (a) $x_1(t)$, $\hat{x}_1(t)$; (b) $x_2(t)$, $\hat{x}_2(t)$; (c) $x_3(t)$, $\hat{x}_3(t)$

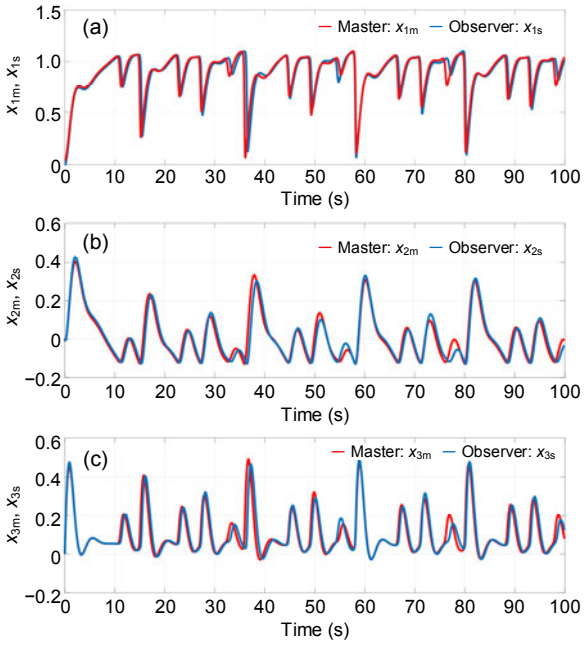

Fig. 5 Evolution of the trajectories when the controller is activated: (a) $x_1(t)$, $\hat{x}_1(t)$; (b) $x_2(t)$, $\hat{x}_2(t)$; (c) $x_3(t)$, $\hat{x}_3(t)$

For clarity, we adopt subscripts "m" and "s" to denote the master and the observer system trajectories, respectively. It seems that the trajectories diverge after a long, irregular, transient oscillation. This is due to the complex environment considered in this approach. Note that the transient period shows apparent synchronization as observed in any physical system that is subjected to external disturbances and uncertainties. These undesirable features are often probabilistic and cannot be handled by the designer to control an automatic scheme.

To design the controller and provide a criterion for ensuring robust passivity based on the synchronization of the drive-response system, we select the following initial conditions: $(k_{11}(0), k_{12}(0), k_{13}(0))=(10^{-4}, 1.41\times10^{-7}, 4.51\times10^{-7})$ and $\gamma=5\times10^{-3}$. Fig. 5 shows the state variable trajectories of the master and observer systems. We observe that these systems approach synchronization after a short transient time. The novelty of this control scheme is linked to many control gains and the associated adaptation gain schedule. The principle of passivity used in this context provides a powerful tool to improve the robustness of the control system with many sources of disturbance.

Fig. 6 depicts the controller gains $K_{11}(t)$. Note that the optimum value of the gain matrix $(K_{11})_{\max}$ cannot be reached, so complete synchronization is achieved partially. The number of variations of the matrix elements that allow the designer to execute the system physically is very small, which demonstrates how effective the synchronization is.

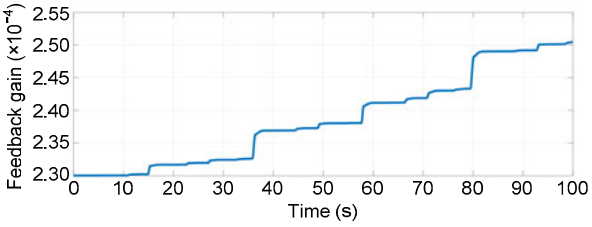

Fig. 6 Time evolution of the feedback gains $K_{11}(t)$

Performance indices are considered to determine the performance of the control system, such as the integral of a squared error (ISE) and the integral of an absolute error (IAE) (Tavazoei, 2010). A general form of the integral index is defined by

$$I(r,s)=\int_0^{\infty} t^r \left(\sum_{i=1}^{n} e_i^2(t)\right)^s \mathrm{d}t, \tag{63}$$

where r and s are set as follows: r=0 and s=1 for IAE; r=1 and s=2 for ISE. The quadratic gap of the corresponding synchronization process can be evaluated as

$$\mathrm{ISE}=I(1,2)=(t+0.001)^{-1}\int_0^t\left|e_q(\theta)\right|^2\mathrm{d}\theta. \quad (64)$$

Fig. 7 depicts the performance index of the synchronization.

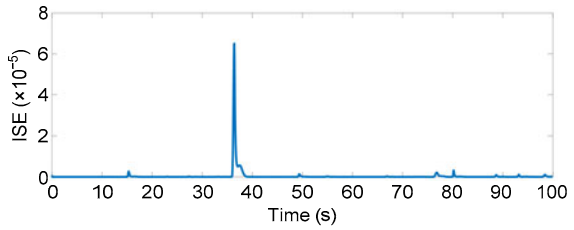

Fig. 7 Performance index of the synchronization (ISE: integral of a squared error)

Remark 3 (Comparative analysis) Let us point out some promising results obtained in the literature using similar approaches. Dadras and Momeni (2013) discussed the problem of designing a passivity-based fractional-order integral sliding mode controller for uncertain fractional-order nonlinear systems using the passivity definition of integer-order systems. We note that the dissipative inequality in the definition of dissipativity of integer-order systems cannot characterize the memory property of the fractional energy dissipation of fractional-order systems. The same results were obtained by Song S et al. (2017) and Chen et al. (2019) using the LMI approach for the passive projective synchronization associated with uncertain systems and the LMI technique for robust passivity for linear systems, respectively. Although good results have been obtained, the following should be considered: (1) the feedback gain is high which characterizes the effort supplied by the scheme to achieve synchronization; (2) the LMI approach used in many papers renders the controller complex in its topological form, and consequently its physical implementation boring. In this work, the observer is robust and allows the scheme to reach synchronization faster with respect to the approach proposed by Kammogne et al. (2013).

4.3 Reduction of the size of the feedback coupling controller

The special aspect provided in this work is that there is a real possibility of choosing large observer gains such that the linear part overcomes nonlinear ones. These quantities are known as high-gain observers (Gauthier et al., 1992; Nijmeijer and Mareels, 1997; Feki, 2003; Noube et al., 2013). This approach can be applied in any dynamic system. This subsection deals with the specific case linked to a topological property of the systems. We will show that the minimum phase characteristic of the Colpitts system, as defined in Assumption 1, allows the size of the feedback coupling controller to be reduced.

The presence of the controller in each observer equation remains a major drawback of the polynomial controller, because knowledge of all states is not necessary in the question of synchronization.

Theorem 4 The Colpitts system satisfies the minimum phase property. Hence, when the single controlled state converges to zero, the other uncontrolled system states also stabilize at the origin. Therefore, only the first state of the slave system should be controlled to achieve complete synchronization.

Proof The synchronization error dynamics can be written in the following detailed form:

$$\dot{e}_1^{q_1}=\Delta F+u_1,\ \dot{e}_2^{q_2}=-\beta e_2+e_3,\ \dot{e}_3^{q_3}=-e_1-e_2-\gamma e_3,$$

where

$$\Delta F=e_3+\left[(-\alpha \mathrm{e}^{-a\hat{x}_3-b\hat{x}_2})-(-\alpha \mathrm{e}^{-ax_3-bx_2})\right].$$

Note that the feedback coupling controller is applied only on the first state variable. Hence, for m=2, controller (56) can be simplified as follows:

$$u_1=-k_{11}(e_1-e_3)-k_{21}(e_1-e_3)^3. \quad (65)$$

The adaptive feedback gain in Eq. (57) can be simplified as

$$k_{11}=k_{11}(0)e_1^2. \quad (66)$$

To demonstrate that the error system is at the minimum phase, we must show that $\dot{e}_2^{q_2}=-\beta e_2+e_3$ and $\dot{e}_3^{q_3}=-e_1-e_2-\gamma e_3$ converge asymptotically to the origin when e_1=0. The dynamics of the two uncontrolled error subsystems can be written as

$$\dot{\boldsymbol{e}}^q=\boldsymbol{E}\boldsymbol{e}, \quad (67)$$

where $\boldsymbol{E}=\begin{bmatrix}-\beta & 1\\ -1 & -\gamma\end{bmatrix}$ and $\boldsymbol{e}=\begin{bmatrix}e_2\\ e_3\end{bmatrix}$.

Note that matrix $\boldsymbol{E}$ is Hurwitz because its trace is negative and its determinant is positive (i.e., tr($\boldsymbol{E}$)=$-\beta-\gamma<0$ and det($\boldsymbol{E}$)=$\beta\gamma+1>0$). Hence, error subsystem $\dot{\boldsymbol{e}}^q=\boldsymbol{E}\boldsymbol{e}$ is asymptotically stable, and system (53) is a minimum-phase one. So, when we apply feedback coupling on the first state variable of the observer (slave system) to achieve $e_1(t)=0$, the other uncontrolled states ($e_2(t)$, $e_3(t)$) will converge to zero when $t\to\infty$ for the so-called minimum-phase behavior. Fig. 8 depicts the trajectories of the master-slave systems when the reduced controller is applied.

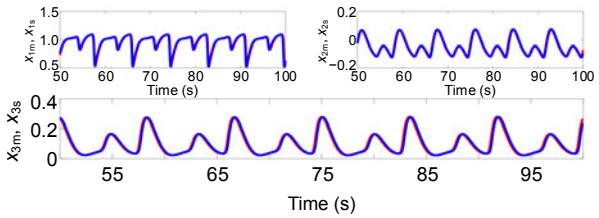

Fig. 8 Trajectory states of the master and the slave for the passive controller (53) when q=0.9

4.4 Implementation scheme of the polynomial observer for passive synchronization

The corresponding circuit diagram of the FMCO is sketched in Fig. 9, for the master system and slave system. A detailed description of this circuit in integer order has been studied in detail by Kammogne et al. (2013).

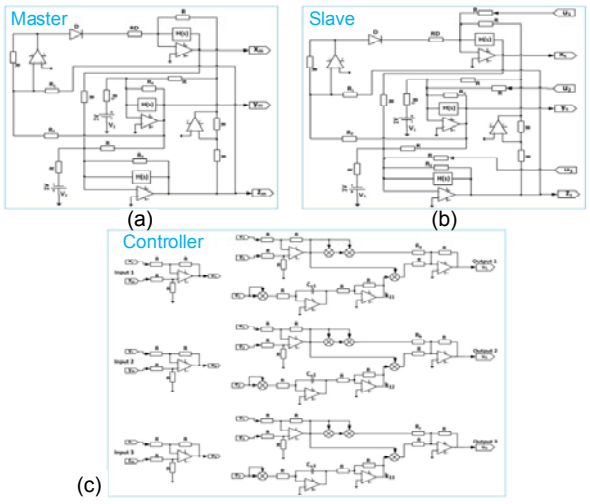

Fig. 9 Equivalent model of the fractional-order modified Colpitts oscillator (FMCO) view as a master system (a), circuit implementation of the slave system (b), and circuit implementation of the feedback coupling controller given by Eqs. (56) and (57) (c)

This circuit allows the current to be regulated by the inductor. The component values are chosen as $I_0=10^{-12}$ A, V_T=0.026 V, R=10 kΩ, R_d=117.39 Ω, R_1=170.837 kΩ, R_2=2 kΩ, R_3=R_4=93.913 kΩ, R_5=10.7 kΩ, V_1=V_2=1 V, R_a=666.66 kΩ, R_b=1.66 MΩ, R_c=883.33 kΩ. The complete circuit is supplied with V^+=+15 V and V^-=−15 V. Fig. 9c presents the controller.

The constant parameters of the polynomial controller (56) are calculated as follows:

$$k_{21}=R/R_a,\ k_{22}=R/R_b,\ k_{23}=R/R_c. \tag{68}$$

In this subsection, we analyze the effect of fractional order on passive synchronization of the FMCO by the polynomial robust observer.

Case 1: q=1. Fig. 10 shows the synchronization error. After a short transient time, the master and the slave systems reach synchronization. Note that during

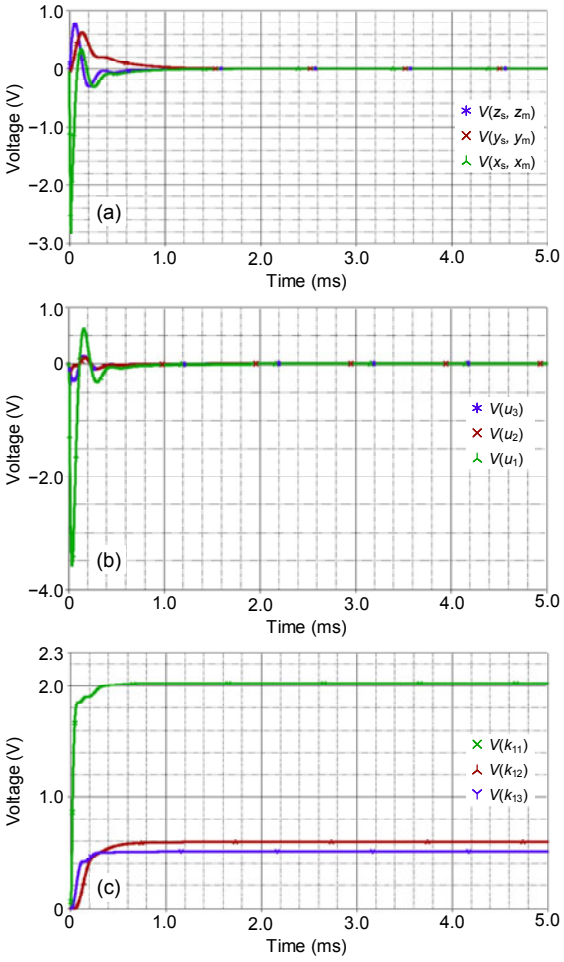

Fig. 10 Time evolution of the synchronization errors (a), feedback coupling controllers u_1, u_2, and u_3 (b), and feedback gains k_{11}, k_{12}, and k_{13} (c) when q=1

the synchronization process, the master system remains chaotic. Fig. 11 shows this behavior.

Case 2: q=0.98. The PSpice results from this derivative order are presented in Fig. 12.

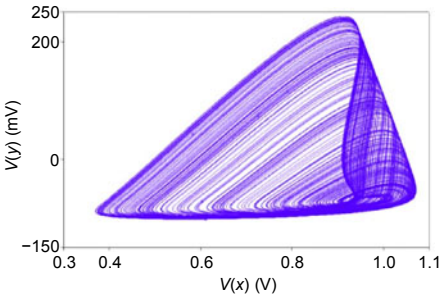

Fig. 11 Phase portraits corresponding to the master system during synchronization when q=1

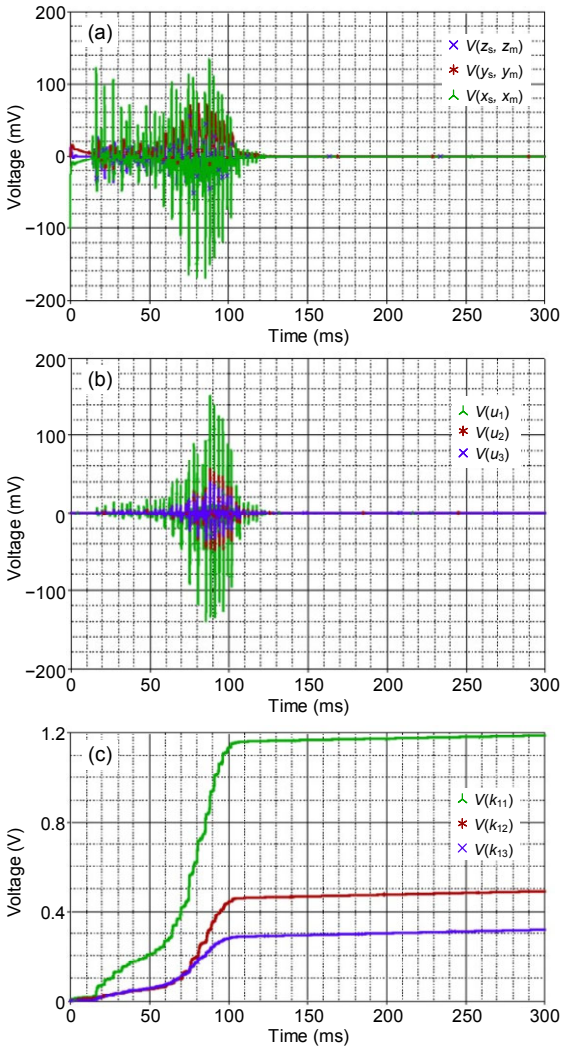

Fig. 12 Time evolution of the synchronization errors (a), feedback coupling controllers u_1, u_2, and u_3 (b), and feedback gains k_{11}, k_{12}, and k_{13} (c) when q=0.98

Case 3: q=0.95. The results for this case are presented in Fig. 13.

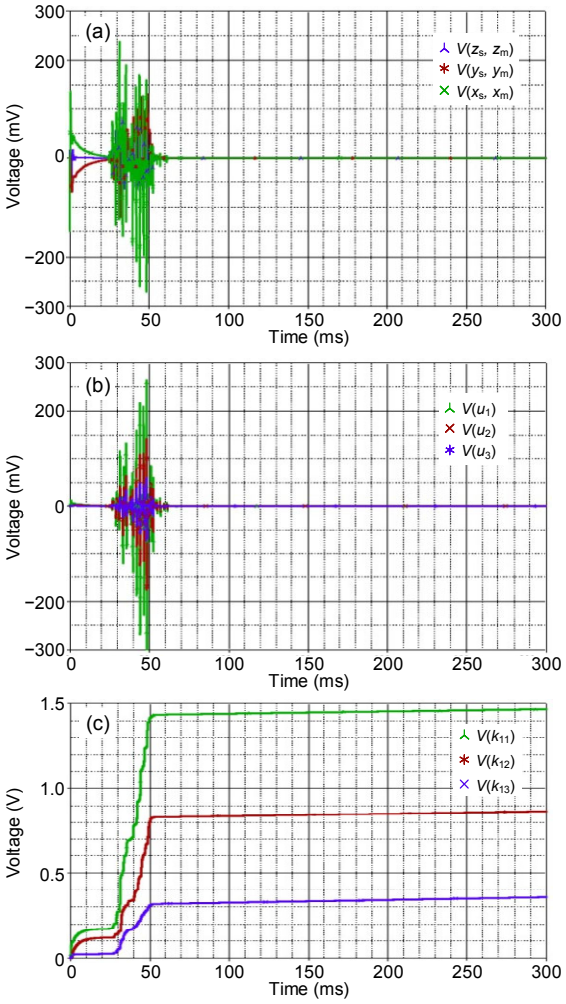

Fig. 13 Time evolution of the synchronization errors (a), feedback coupling controllers u_1, u_2, and u_3 (b), and feedback gains k_{11}, k_{12}, and k_{13} (c) when q=0.95

The circuit implementation of the integral operator is the key point of designing a fractional-order chaotic circuit. The standard definition of a fractional differintegral does not allow direct implementation of the fractional operators in time-domain simulations. The approximate formula of the fractional order using the integer operator was designed in Liu (2011) and Hammouch and Mekkaoui (2018). The main characteristics of these results are summarized in Table 1 for two derivative orders (q=0.95, 0.98).

Table 1 Fractional-order chains with their corresponding values

Derivative order	Component values	Transfer function	Electric diagram
q=0.98	R_{f1}=91.19 MΩ R_{f2}=190.09 MΩ C_{f1}=60.93 nF C_{f2}=230 nF	$H(s)$	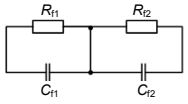
q=0.95	R_{f3}=15.1 kΩ R_{f4}=1.51 MΩ R_{f5}=692 MΩ C_{f3}=227 nF C_{f4}=287 nF C_{f5}=80 nF	$H(s)$	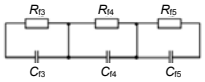

4.5 Reduced passive feedback coupling controller on PSpice

In this case, we consider the derivative order 0.95. Taking into account Eqs. (65) and (66), we derive the passive controller diagram shown in Fig. 14.

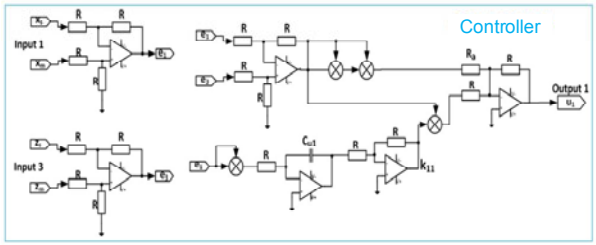

Fig. 14 Circuit implementation of the feedback coupling controller given by Eqs. (65) and (66)

The PSpice results of the controlled fractional-order Colpitts system are shown in Figs. 15a and 15b. These figures show that synchronization is achieved after a long period. Compared with Figs. 12 and 13, we observe that the transient period for the reduced passive feedback coupling (T_{rpf}) for synchronization is twice that of the initial polynomial observer (T_{po}), or $T_{\mathrm{rpf}}\approx 2T_{\mathrm{po}}$. This feature is a drawback of the reduced feedback coupling. Fig. 15c depicts the adaptive control law of controller $u_1(t)$. It is observed that the control effort, which is measured by $\int_0^{\infty} u_1(t)\mathrm{d}t$, is quite similar to the previous results. From the above results, the response system of the fractional-order Colpitts chaotic system is synchronized with the observer and has good control performance.

Remark 4 From PSpice results, it is obvious that the convergence rate of the fractional synchronization error deserves an additional definition. Indeed, in many studies, researchers have shown indubitably that the convergence of the synchronized states of fractional systems is faster than that of their counterparts with integer-order derivatives (Aghababa, 2012a; Kuntanapreeda, 2016). Our results show the opposite. This is due to the physical nature of the polynomial controller, and more precisely the concept of passivity with which it is associated. The variation of the curve in Fig. 7 does not describe an exponential decay compared to the work presented in Kammogne et al. (2019). These characteristics of the control scheme ensure slower decay compared with those usually encountered in the literature.

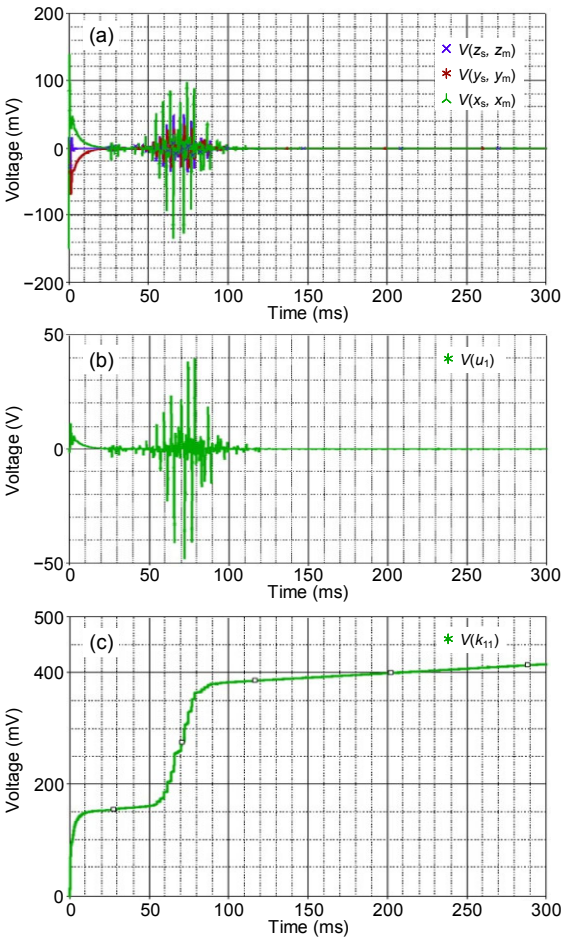

Fig. 15 Time evolution of synchronization errors (a), feedback coupling controller u_1 (b), and feedback gain k_{11} (c)

Remark 5 Passivity remains an important characteristic of controllers interacting with uncertain systems. The controller assures the relation between external force $\xi(t)$ and the system states, which yields stable behavior in free motion. Figs. 10b, 12b, 13b, and 15b show the stabilization of the controller to the origin. When the systems reach synchronization, the effect of the controller vanishes. These results strongly illustrate the passivity concept presented in Definition 2.

5 Conclusions

In this paper we have proposed robust observer strategy based passive synchronization for two chaotic fractional-order systems (FOSs) with structural disturbances. We designed a polynomial robust observer in terms of the adaptive control theory and the concept of passivity. Based on the Lyapunov stability theory and Finsler's lemma, sufficient conditions were derived for stability of closed-loop systems. A special case based on the minimum-phase properties of Colpitts oscillators was also considered and the practicable robust observer derived. The proposed approach allows us to establish a typical procedure for analysis of stability in chaotic FOSs. PSpice's implementation showed that our approach is not limited to numerical simulations, but offers important computational methods for the design of a passive controller in real time. An illustrative example was used to test the efficiency of the proposed solution, which offers strong robustness properties against structural uncertainty and unmodeled dynamics. The efficiency of our methodology is of great significance for applications in the real world.

Contributors

Alain Soup Tewa KAMMOGNE conceived and designed the research, contributed reagents, analysis tools or data, and interpreted the data. Ahmad Taher AZAR contributed reagents, materials, analysis tools or data. Michaux Noubé KOUNTCHOU, Romanic KENGNE, and Soup Teoua Michael OUAGNI performed the experiments. Michaux Noubé KOUNTCHOU analyzed the data. Alain Soup Tewa KAMMOGNE and Soup Teoua Michael OUAGNI drafted the paper. Alain Soup Tewa KAMMOGNE, Hilaire Bertrand FOTSIN, and Ahmad Taher AZAR revised and finalized the paper.

Acknowledgements

We thank Prince Sultan University, Riyadh, Saudi Arabia for supporting this research. Our gratitude also goes to Robotics and Internet-of-Things Lab (RIOTU), Prince Sultan University, Riyadh, Saudi Arabia. Reviewers' valuable comments have improved the presentation of this paper.

Compliance with ethics guidelines

Alain Soup Tewa KAMMOGNE, Michaux Noubé KOUNTCHOU, Romanic KENGNE, Ahmad Taher AZAR, Hilaire Bertrand FOTSIN, and Soup Teoua Michael OUAGNI declare that they have no conflict of interest.

References

Aghababa MP, 2012a. Finite-time chaos control and synchronization of fractional-order nonautonomous chaotic (hyperchaotic) systems using fractional nonsingular terminal sliding mode technique. *Nonl Dynam*, 69(1):247-261. https://doi.org/10.1007/s11071-011-0261-6

Aghababa MP, 2012b. Robust finite-time stabilization of fractional-order chaotic systems based on fractional Lyapunov stability theory. *J Comput Nonl Dynam*, 7(2): 021010. https://doi.org/10.1115/1.4005323

Aghababa MP, 2014. Control of fractional-order systems using chatter-free sliding mode approach. *J Comput Dynam*, 9(3):031003. https://doi.org/10.1115/1.4025771

Aghababa MP, 2015a. A fractional sliding mode for finite-time control scheme with application to stabilization of electrostatic and electromechanical transducers. *Appl Math Model*, 39(20):6103-6113. https://doi.org/10.1016/j.apm.2015.01.053

Aghababa MP, 2015b. Synchronization and stabilization of fractional second-order nonlinear complex systems. *Nonl Dynam*, 80(4):1731-1744. https://doi.org/10.1007/s11071-014-1411-4

Ammar HH, Azar AT, Shalaby R, et al., 2019. Metaheuristic optimization of fractional order incremental conductance (FO-INC) maximum power point tracking (MPPT). *Complexity*, 2019:7687891. https://doi.org/10.1155/2019/7687891

Azar AT, Vaidyanathan S, Ouannas A, 2017a. Fractional Order Control and Synchronization of Chaotic Systems. Springer, Cham, Germany. https://doi.org/10.1007/978-3-319-50249-6

Azar AT, Volos C, Gerodimos NA, et al., 2017b. A novel chaotic system without equilibrium: dynamics, synchronization, and circuit realization. *Complexity*, 2017:7871467. https://doi.org/10.1155/2017/7871467

Azar AT, Radwan AG, Vaidyanathan S, 2018a. Fractional Order Systems: Optimization, Control, Circuit Realizations and Applications. Elsevier, Amsterdam, the Netherlands. https://doi.org/10.1016/C2017-0-04459-2

Azar AT, Radwan AG, Vaidyanathan S, 2018b. Mathematical Techniques of Fractional Order Systems. Elsevier, Amsterdam, the Netherlands. https://doi.org/10.1016/C2016-0-05031-3

Byrnes CI, Isidori A, Willems JC, 1991. Passivity, feedback equivalence, and the global stabilization of minimum phase nonlinear systems. *IEEE Trans Autom Contr*, 36(11):1228-1240. https://doi.org/10.1109/9.100932

Chen LP, Chai Y, Wu RC, et al., 2012. Cluster synchronization in fractional-order complex dynamical networks. *Phys Lett A*, 376(35):2381-2388. https://doi.org/10.1016/j.physleta.2012.05.060

Chen LP, Li TT, Chen YQ, et al., 2019. Robust passivity and feedback passification of a class of uncertain fractional-order linear systems. *Int J Syst Sci*, 50(6):1149-1162. https://doi.org/10.1080/00207721.2019.1597940

Cho YM, Rajamani R, 1997. A systematic approach to adaptive observer synthesis for nonlinear systems. *IEEE Trans Autom Contr*, 42(4):534-537. https://doi.org/10.1109/9.566664

Dadras S, Momeni HR, 2013. Passivity-based fractional-order integral sliding-mode control design for uncertain fractional-order nonlinear systems. *Mechatronics*, 23(7): 880-887. https://doi.org/10.1016/j.mechatronics.2013.05.009

Dasgupta T, Paral P, Bhattacharya S, 2015. Fractional order sliding mode control based chaos synchronization and secure communication. Proc Int Conf on Computer Communication and Informatics, p.8-10. https://doi.org/10.1109/iccci.2015.7218161

de Oliveira MC, Skelton RE, 2000. Stability tests for constrained linear systems. In: Moheimani SOR (Ed.), Perspectives in Robust Control. Springer, London, UK. p.241-257. https://doi.org/10.1007/BFb0110624

Diethelm K, Ford NJ, Freed AD, 2002. A predictor-corrector approach for the numerical solution of fractional differential equations. *Nonl Dynam*, 29(1-4):3-22. https://doi.org/10.1023/A:1016592219341

Djeddi A, Dib D, Azar AT, et al., 2019. Fractional order unknown inputs fuzzy observer for Takagi-Sugeno systems with unmeasurable premise variables. *Mathematics*, 7(10): 984. https://doi.org/10.3390/math7100984

Feki M, 2003. Observer-based exact synchronization of ideal and mismatched chaotic systems. *Phys Lett A*, 309(1-2): 53-60. https://doi.org/10.1016/S0375-9601(03)00171-3

Fotsin HB, Daafouz J, 2005. Adaptive synchronization of uncertain chaotic colpitts oscillators based on parameter identification. *Phys Lett A*, 339(3-5):304-315. https://doi.org/10.1016/j.physleta.2005.03.049

Gai MJ, Cui SW, Liang S, et al., 2016. Frequency distributed model of Caputo derivatives and robust stability of a class of multi-variable fractional-order neural networks with uncertainties. *Neurocomputing*, 202:91-97. https://doi.org/10.1016/j.neucom.2016.03.043

Gauthier JP, Hammouri H, Othman S, 1992. A simple observer for nonlinear systems applications to bioreactors. *IEEE Trans Autom Contr*, 37(6):875-880. https://doi.org/10.1109/9.256352

Ghoudelbourk S, Dib D, Omeiri A, et al., 2016. MPPT control in wind energy conversion systems and the application of fractional control (PI^{α}) in pitch wind turbine. *Int J Model Ident Contr*, 26(2):140-151. https://doi.org/10.1504/IJMIC.2016.078329

Hammouch Z, Mekkaoui T, 2018. Circuit design and simulation for the fractional-order chaotic behavior in a new dynamical system. *Compl Intell Syst*, 4(4):251-260. https://doi.org/10.1007/s40747-018-0070-3

Issakhov A, Baitureyeva AR, 2018. Numerical modelling of a passive scalar transport from thermal power plants to air environment. *Adv Mech Eng*, 10(10):1-14. https://doi.org/10.1177/1687814018799544

Kammogne ST, Fotsin HB, 2014. Adaptive control for modified projective synchronization-based approach for estimating all parameters of a class of uncertain systems: case of modified Colpitts oscillators. *J Chaos*, 2014:659647. https://doi.org/10.1155/2014/659647

Kammogne ST, Fotsin HB, Kountchou NM, et al., 2013. A robust observer design for passivity-based synchronization of uncertain modified Colpitts oscillators and circuit simulation. *Asian J Sci Technol*, 5(1):29-41.

Kammogne AST, Azar AT, Bertrand FH, et al., 2019. Robust observer-based synchronisation of chaotic oscillators with structural perturbations and input nonlinearity. *Int J Autom Contr*, 13(4):387-412. https://doi.org/10.1504/IJAAC.2019.100467

Kammogne AST, Azar AT, Kengne R, et al., 2020. Stability analysis and robust synchronisation of fractional-order modified Colpitts oscillators. *Int J Autom Contr*, 14(1):52-79. https://doi.org/10.1504/IJAAC.2020.103806

Kengne R, Tchitnga R, Mabekou S, et al., 2018. On the relay coupling of three fractional-order oscillators with time-delay consideration: global and cluster synchronizations. *Chaos Sol Fract*, 111:6-17. https://doi.org/10.1016/j.chaos.2018.03.040

Khalil HK, 2007. Nonlinear Systems (3rd Ed.). Prentice Hall, Upper Saddle River, New Jersey, USA.

Khan A, Singh S, Azar AT, 2020a. Combination-combination anti-synchronization of four fractional order identical hyperchaotic systems. Int Conf on Advanced Machine Learning Technologies and Applications, p.406-414. https://doi.org/10.1007/978-3-030-14118-9_41

Khan A, Singh S, Azar AT, et al., 2020b. Synchronization between a novel integer-order hyperchaotic system and a fractional-order hyperchaotic system using tracking control. Proc 10th Int Conf on Modelling, Identification and Control, p.382-391. https://doi.org/10.1109/ICMIC.2018.8529895

Kuntanapreeda S, 2016. Adaptive control of fractional-order unified chaotic systems using a passivity-based control approach. *Nonl Dynam*, 84(4):2505-2515. https://doi.org/10.1007/s11071-016-2661-0

Li C, Xiong J, Li W, et al., 2013. Robust synchronization for a class of fractional-order dynamical system via linear state variable. *Ind J Phys*, 87(7):673-678. https://doi.org/10.1007/s12648-013-0267-7

Li CP, Deng WH, 2007. Remarks on fractional derivatives. *Appl Math Comput*, 187(2):777-784. https://doi.org/10.1016/j.amc.2006.08.163

Li LL, Yao QG, 2014. Robust synchronization of chaotic systems using sliding mode and feedback control. *J Zhejiang Univ-Sci C (Comput & Electron)*, 15(3):211-222. https://doi.org/10.1631/jzus.C1300266

Li TZ, Wang Y, Zhao C, 2017. Synchronization of fractional chaotic systems based on a simple Lyapunov function. *Adv Differ Equat*, 2017(1):304. https://doi.org/10.1186/s13662-017-1320-1

Liu CX, 2011. Fractional-Order Chaotic Circuit Theory and Applications. Xi'an Jiaotong University Press, Xi'an, China (in Chinese).

Ngouonkadi EBM, Fotsin HB, Fotso PL, 2014. Implementing a memristive Van der Pol oscillator coupled to a linear oscillator: synchronization and application to secure communication. *Phys Scr*, 89(3):035201. https://doi.org/10.1088/0031-8949/89/03/035201

Nijmeijer H, Mareels IMY, 1997. An observer looks at synchronization. *IEEE Trans Circ Syst I*, 44(10):882-890. https://doi.org/10.1109/81.633877

Noube MK, Louodop P, Bowong S, et al., 2013. Optimization of the synchronization of the modified Duffing system. *J Adv Res Dynam Contr Syst*, 6(2):1-24.

Noun S, Botmart T, 2018. New results on passivity criteria for a class of neural networks with interval and distributed time-varying delays. Proc Int Multiconf of Engineers and Computer Scientists.

Pecora LM, Carroll TL, 1990. Synchronization in chaotic systems. *Phys Rev Lett*, 64(8):821-824. https://doi.org/10.1103/PhysRevLett.64.821

Pelap FB, Tanekou GB, Fogang CF, et al., 2018. Fractional-order stability analysis of earthquake dynamics. *J Geophys Eng*, 15(4):1673-1687. https://doi.org/10.1088/1742-2140/aabe61

Podlubny I, 1999. Fractional Differential Equations. Academic Press, San Diego, CA, USA.

Qi WH, Gao XW, Wang JY, 2016. Finite-time passivity and passification for stochastic time-delayed Markovian switching systems with partly known transition rates. *Circ Syst Signal Process*, 35(11):3913-3934. https://doi.org/10.1007/s00034-015-0239-6

Rabah K, Ladaci S, Lashab M, 2018. Bifurcation-based fractional-order $PI^{\lambda}D^{\mu}$ controller design approach for nonlinear chaotic systems. *Front Inform Technol Electron Eng*, 19(2):180-191. https://doi.org/10.1631/FITEE.1601543

Rajavel S, Samidurai R, Cao JD, et al., 2017. Finite-time non-fragile passivity control for neural networks with time-varying delay. *Appl Math Comput*, 297:145-158. https://doi.org/10.1016/j.amc.2016.10.038

Sabatier J, Farges C, 2017. Analysis of fractional models physical consistency. *J Vibr Contr*, 23(6):895-908. https://doi.org/10.1177/1077546315587177

Shen J, Lam J, 2014. H_∞ model reduction for positive fractional order systems. *Asian J Contr*, 16(2):441-450. https://doi.org/10.1002/asjc.694

Skelton RE, Iwasaki T, Grigoriadis KM, 1998. A Unified Algebraic Approach to Linear Control Design. Taylor & Francis, London, UK.

Song J, He SP, 2015. Finite-time robust passive control for a class of uncertain Lipschitz nonlinear systems with time-delays. *Neurocomputing*, 159:275-281. https://doi.org/10.1016/j.neucom.2015.01.038

Song QK, Wang ZD, 2010. New results on passivity analysis of uncertain neural networks with time-varying delays. *Int J Comput Math*, 87(3):668-678. https://doi.org/10.1080/00207160802166507

Song S, Song XN, Balsera IT, 2017. Mixed H_∞ and passive projective synchronization for fractional-order memristor-based neural networks with time delays via adaptive sliding mode control. *Mod Phys Lett B*, 31(14): 1750160. https://doi.org/10.1142/S0217984917501603

Sun D, Naghdy F, Du HP, 2017. Neural network-based passivity control of teleoperation system under time-varying delays. *IEEE Trans Cybern*, 47(7):1666-1680. https://doi.org/10.1109/TCYB.2016.2554630

Tavazoei MS, 2010. Notes on integral performance indices in fractional-order control systems. *J Process Contr*, 20(3): 285-291. https://doi.org/10.1016/j.jprocont.2009.09.005

Tavazoei MS, Haeri M, 2007. A necessary condition for double scroll attractor existence in fractional-order systems. *Phys Lett A*, 367(1-2):102-113. https://doi.org/10.1016/j.physleta.2007.05.081

Tavazoei MS, Haeri M, 2008. Chaotic attractors in incommensurate fractional order systems. *Phys D*, 237(20): 2628-2637. https://doi.org/10.1016/j.physd.2008.03.037

Thuan MV, Huong DC, Hong DT, 2019. New results on robust finite-time passivity for fractional-order neural networks with uncertainties. *Neur Process Lett*, 50(2):1065-1078. https://doi.org/10.1007/s11063-018-9902-9

Vaidyanathan S, Azar AT, 2015a. Anti-synchronization of identical chaotic systems using sliding mode control and an application to Vaidyanathan-Madhavan chaotic systems. In: Azar AT, Zhu QM (Eds.), Advances and Applications in Sliding Mode Control Systems. Springer, Cham, Germany, p.527-547. https://doi.org/10.1007/978-3-319-11173-5_19

Vaidyanathan S, Azar AT, 2015b. Hybrid synchronization of identical chaotic systems using sliding mode control and an application to Vaidyanathan chaotic systems. In: Azar AT, Zhu QM (Eds.), Advances and Applications in Sliding Mode Control Systems. Springer, Cham, Germany, p.549-569. https://doi.org/10.1007/978-3-319-11173-5_20

Vaidyanathan S, Azar AT, 2016a. Qualitative study and adaptive control of a novel 4-D hyperchaotic system with three quadratic nonlinearities. In: Azar AT, Vaidyanathan S (Eds.), Advances in Chaos Theory and Intelligent Control. Springer, Cham, Germany, p.179-202. https://doi.org/10.1007/978-3-319-30340-6_8

Vaidyanathan S, Azar AT, 2016b. Generalized projective synchronization of a novel hyperchaotic four-wing system via adaptive control method. In: Azar AT, Vaidyanathan S (Eds.), Advances in Chaos Theory and Intelligent Control. Springer, Cham, Germany, p.275-296. https://doi.org/10.1007/978-3-319-30340-6_12

Vaidyanathan S, Sampath S, Azar AT, 2015. Global chaos synchronisation of identical chaotic systems via novel sliding mode control method and its application to Zhu system. *Int J Model Ident Contr*, 23(1):92-100. https://doi.org/10.1504/IJMIC.2015.067495

Vaidyanathan S, Azar AT, Akgul A, et al., 2019. A memristor-based system with hidden hyperchaotic attractors, its circuit design, synchronisation via integral sliding mode control and an application to voice encryption. *Int J Autom Contr*, 13(6):644-667. https://doi.org/10.1504/IJAAC.2019.102665

Wang JW, Ma QH, Zeng L, 2013. Observer-based synchronization in fractional-order leader-follower complex networks. *Nonl Dynam*, 73(1-2):921-929. https://doi.org/10.1007/s11071-013-0843-6

Zhang RX, Yang SP, 2013. Robust synchronization of two different fractional-order chaotic systems with unknown parameters using adaptive sliding mode approach. *Nonl Dynam*, 71(1):269-278. https://doi.org/10.1007/s11071-012-0659-9